Renewable Energy 106 (2017) 24–36

Contents lists available at ScienceDirect

Renewable Energy

journal homepage: www.elsevier.com/locate/renene

CFD and experimental investigation of flat plate solar water heating system under steady state condition

Dawit Gudeta Gunjo, Pinakeswar Mahanta, P.S. Robi*

Department of Mechanical Engineering, Indian Institute of Technology Guwahati, Guwahati, 781039, Assam, India

ARTICLE INFO

Article history:
Received 6 July 2016
Received in revised form
15 December 2016
Accepted 16 December 2016
Available online 18 December 2016

Keywords:
Absorber plate temperature
CFD
Outlet temperature
Solar thermal flat plate collector
Thermal performance

ABSTRACT

The absorber plate and outlet water temperature of a solar flat plate collector with straight riser and header arrangement is investigated. The effect of different operating parameters, *viz*., inlet water temperature, solar insolation, ambient temperature, and mass flow rate on the outlet water temperature and thermal efficiency were studied. Both the closed as well as open loop solar water heating system is considered for the present investigation. It is observed that the thermal efficiency of the solar water heating system increases with ambient temperature, solar insolation, and mass flow rate of water. However, thermal efficiency decreases as inlet water temperature increases. Numerical simulations were carried out using a 3-dimensional computational fluid dynamics (CFD) to predict the outlet water and absorber plate temperatures using the experimental values of solar insolation, ambient temperature and inlet water temperature within one hour interval. The CFD results were validated with the experimental results. It was found that the developed model could predict the outlet water and absorber plate temperature of the heating system with reasonable accuracy.

1. Introduction

The energy demands for the last two centuries are mainly by utilizing carbon fuels. Due to the forecast of fossil fuel depletion, researchers are focusing their attention on other energy sources like nuclear energy and non-conventional energy. The increasing environmental concern regarding global warming and the harmful effect of carbon emission, have created a new demand for clean and sustainable energy, *viz*., solar, wind, biomass and geothermal sources of energy. Solar energy is widely accepted as a clean, climate friendly, cheap and limitless energy resource to mankind, relatively well spread over the globe [1]. Among these, the solar energy appears to be most promising alternative in terms of large scale usage at a cheaper rate [2].

Bilgen and Bakeka [3] fabricated a solar water heater and estimated its cost and thermal efficiency. Solar water heating devices are very common systems that are used in many countries which have higher solar radiation, especially Mediterranean countries [4]. Exploiting solar energy for heating requires the use of flat-plate collector systems which receive the incoming solar radiation and then delivers a large fraction of the thermal energy to the working fluids. Solar flat plate collector with metal absorber plate and covers are the most successful devices that convert solar energy in to heat at reasonable price without affecting environment [5,6]. Kalogirou [7] studied the effect of various factors that affects system performance and reported that the collector performance depends on collector construction, arrangement of the collector and collector tilt angle.

In order to improve the efficiency of solar flat plate collector, the convective and radiative heat loss from the front and the back surface of the collector should be minimum. In most commercial flat plate collector the heat losses (33–50%) occurs due to convective losses (22–30%), radiative losses (5–7%) from the absorber front surface, and radiative losses (5–10%) from back surface [8]. Glass is a common choice as a cover for solar thermal devices since it absorbs almost all the infrared radiation re-emitted by the absorber plate thereby enhancing the thermal efficiency of the solar collector and reducing the greenhouse effect. During the design of flat plate solar collector components, care should be given to the number and nature of the transparent covers and on the selectivity of the absorber plate materials [9].

Investigations by Madhukeshwara et al. [10] and Prakash et al. [11] revealed that using special surface coatings increases the incident solar radiation and heat resistance property of material

* Corresponding author.
E-mail address: psr@iitg.ernet.in (P.S. Robi).

http://dx.doi.org/10.1016/j.renene.2016.12.041
0960-1481/

thereby enhancing the operating temperatures. Zambolin and Del Col [12] conducted experimental investigation to study the thermal performance of flat plate and evacuated tube solar water heater. The results indicated that the performance of evacuated solar collector were better than flat plate collector under the same conditions.

Hottel and Woertz [13] conducted the first study on heat transfer coefficient in a flat plate solar collector by means of lumped system analysis. Duffle and Beckman [14] used lumped analysis and found the expression for fluid temperature as well as plate temperature for the solar collector. Gorla [15] performed an analysis based on the two-dimensional finite element method to characterize the performance of solar collectors.

Akhtar and Mullick [16] carried out numerical investigation for double and single-glazed solar collectors. The developed numerical equation was used for calculating the glass temperature at inner and outer surface of the collector for different solar insolation. Lecoeuche and Lalot [17] applied neural network technique to predict the thermal performance of a solar flat plate collector. Amer et al. [18] used a transient testing technique to investigate the effects of inlet water temperature and collector tilt angle on the performance of a solar collector. Shariah and Shalab [19] used TRNSYS (transient simulation program) to optimize design parameters for maximizing the performance of the solar water heater.

Sultana et al. [20] used CFD software to investigate the thermal performance of a solar collector by predicting the heat loss, radiation, and convective heat transfer coefficient inside the collector and maximized the overall thermal efficiency. A numerical study for single glazed flat plate collector was reported by Selmi et al. [21] and CFD software was used to predict outlet water temperature. Their study revealed good agreement between the CFD results and experimental data. Gertzos et al. [22] and Gadi [23] used CFD and found that the developed model predicted system performance with minimal error.

Martinopoulos et al. [24] investigated polymer solar collector using CFD analysis. In their study the effect of operating parameters such as flow rate, temperature, solar insolation, etc. on thermal efficiency were carried out and found good agreement between the experimental and simulation result. Al-Ansary and Zeitoun [25] investigated the parabolic trough collectors using CFD simulation. Numerical modeling was used for calculating the conduction and convective heat losses from the receiver of the collector. Generally, estimation of various parameters under different weather conditions by experiments is time consuming and costly. Use of computational tools prior to the experiments can save a number of experiments and time.

A closed loop and open loop solar water heating system is considered for the present investigation. The closed loop system is utilized to heat the feedstock inside an anaerobic digester for efficient biogas production. In the open loop system, since there is no heat exchanger, the heat is supplied to the digester by manually mixing the hot water from the solar collector with the feedstock outside the biogas digester is mandatory.

The present study is aimed at performance evaluation of the open loop as well closed loop solar water heating systems by carrying out experiments as well as computational technique. A 3-dimensional CFD model is developed to predict the outlet water and absorber plate temperature of the solar water heater. The CFD result is validated with that obtained from experiments. The steady state simulation was carried out using the average values of measured data within one hour interval for a full day experiment. Experiments were carried out under different Guwahati climatic conditions, *viz*., solar insolation, ambient temperature, inlet water temperature, flow rate, and wind speed. The effect of various external parameters on the thermal efficiency and outlet water temperature are also discussed.

1.1. Flat plate collector

The developed flat plate collector used for the present study consists of brazed riser and header pipes, plate material, glass cover, and insulated casing. The brazed riser and header pipe assembly is illustrated in Fig. 1.

It consists of two headers and 10 vertical tube risers. The risers were connected to the headers by drilling and brazing. The absorber plate material consists of copper sheet attached with riser tubes. The surface of the absorber was coated with special coating (90% absorbance and 10% emittance) to maximize the absorbance of the radiant energy. The heat loss due to convection, conduction and re-radiation was reduced by providing an acrylic glass cover at the top of the collector. The bottom and side of the collector was insulated with glass wool and the cold water storage tank was insulated with polyethylene material. The cold water was circulated through the pipes using a 0.25 hp pump. The water flow rate was adjusted by means of a flow control valve. The detailed descriptions of the fabricated collector are shown in Table 1.

1.2. Experimental setup

The experimental setup of the open loop and closed loop solar water heating systems used for the present study are shown in Fig. 2(a) and (b).

The cold water storage tank was insulated and connected to the inlet of the flat plate collector by means of PVC pipes. The outlet from the open loop collector was connected to the hot water storage tank. The cold water from the storage tank was pumped in to the flat plate collector through the bottom part of the header pipe. The inlet water gets heated up during circulation through the riser, which is subsequently stored in the hot water storage tank.

In the closed loop solar water heating system, the water stored in the reservoir tank is circulated in a closed loop manner by passing through the collector, a heat exchanger at the bottom of the storage tank and finally to the reservoir tank. The heat exchanger transfers heat from the collector loop fluid to the water located in the storage tank.

The photograph of the open loop solar heating system indicating position of various sensors and instruments is shown in Fig. 3.

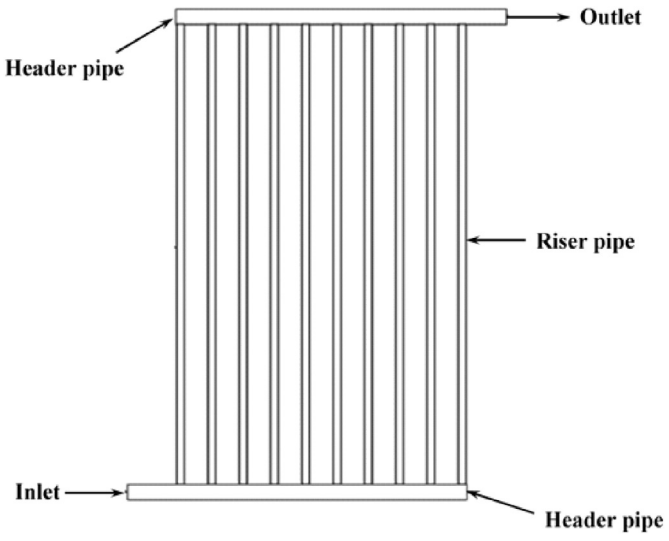

Fig. 1. Schematic diagram of riser and header pipe.

Table 1
Detailed specifications fabricated solar collector.

Description	Specification and type
Length of the collector	1.8 m
Width of the collector	1.2 m
Length of the absorber plate	1.65 m
Width of the absorber plate	1 m
Thermal conductivity of the absorber plate	386 W (m K)$^{-1}$
Density of the plate material	8954 kg m^{-3}
Plate thickness	0.0005 m
Diameter of header pipe	0.025 m
Diameter of riser pipe	0.0125 m
Riser and header pipe thickness	0.0007 m
Tube center to center distance	0.1125 m
Number of glass	1
Spacing between glass and absorber plate	0.03 m
Insulating material	Glass wool
Thermal conductivity of insulation material	0.044 W (m K)$^{-1}$
Thickness of the insulation material	0.04 m
Density of the insulation material	200 kg m^{-3}
Thickness of glazing material	0.03 m

The solar radiation from the collector surface was measured using pyranometer whereas the inlet and outlet water temperatures, ambient temperature, absorber plate temperature and glass temperature were measured using K-type thermocouples. The entire data during the experiment were recorded by a data acquisition system at an interval of 20 s. The solar collector was placed at latitude of 26.13°N and longitude 91.73°E. The experiment was carried out during November–December 2015.

1.3. Methodology

The outlet water and absorber plate temperature of the solar collector depends on the flow distribution in the riser tubes. Flow at low Reynolds number (<0.016 kg s^{-1}) would give uniform flow with homogenous temperature distribution in each riser tubes [26]. The CFD model was developed to predict the outlet and absorber plate temperature for a single straight riser tube attached at the bottom of an absorber plate. The flow rate in each riser tube was 1/10th of the total flow rate in the header tube (i.e., the ratio of the total flow rate through the header tube to the number of riser tubes). Analysis was carried out based on the following assumptions:

- The thermal and physical property of the absorber plate, riser tube and water are constant during the flow.
- Water is incompressible and continuous.
- Heat loss from the bottom side of the absorber plate and tube is by convection which depends upon the wind speed.

Fig. 4 illustrates the model geometry of the computational domain.

For modeling, the absorber plate length, width, tube diameter and tube thickness are 1.65 m, 0.1 m, 0.0125 m and 0.007 m respectively, which is the same dimension of the experimental setup. The data used for the modeling, *viz.*, inlet water temperature, ambient temperature, solar insolation and wind speed is based on the data obtained from few initial experiments. The velocity and temperature field for the water flow in the riser tube and temperature field on the absorber plate is determined by solving the equations of continuity, momentum and energy. The grid independency test was done to check the quality of mesh on the solution. The solutions converged when the values of residuals in the computational domain fell below 1×10^{-6}. Further grid refining resulted in an error less than 0.6%. The number of elements for the computational domain consisting of water, water tube and absorber plate is 400,000. The magnified meshed part of the developed model is shown in Fig. 5.

A constant heat flux (solar irradiance) is applied on the top surface of the absorber plate. The bottom surface is set as convective wall boundary. The convective heat transfer coefficient of the bottom surface is obtained by the expression [27]:

$$h_b = 2.8 + 3V_w \tag{1}$$

The heat energy absorbed by the solar collector is obtained by the expression:

$$Q_i = (\alpha\tau)I \tag{2}$$

The outlet water and absorber plate temperature is computed using general purpose CFD software. The convective heat transfer between the fluid zones and the corresponding faces are solved by coupling the momentum and energy equations. The SIMPLE method is used for the discretization of the pressure and second order upwind for momentum and energy equations.

The efficiency of the solar collector (η) is determined by the expression:

$$\eta = \frac{Q}{IA_c} \tag{3}$$

The heat absorbed by the water is determined by the relationship:

$$Q = \dot{m}C_p(T_o - T_i) \tag{4}$$

The instantaneous solar collector efficiency in terms of inlet and outlet water temperature is determined using eq. (5) which was obtained by substituting eq. (4) in to eq. (3).

$$\eta = \frac{\dot{m}C_p(T_o - T_i)}{IA_c} \tag{5}$$

2. Result and discussion

2.1. Model validation

The input parameter for the computational model was solar radiation (I), ambient temperature (Ta), inlet water temperature (Ti), and mass flow rate. Simulation was carried out for predicting the outlet water temperature (To) and absorber plate temperature (Tp). The steady state simulation conducted in this model used the average values of measured data within one hour interval. Validation of the model was carried out by comparing the simulation results with the experimental values. Figs. 6 and 7 illustrate the results of the experiment carried out using straight tube flat plate collector at flow rates of 0.0125 kg s^{-1} and 0.025 kg s^{-1} respectively, for time periods from 8:00 h to 16:00 h.

The CFD results for variations in outlet water temperature: (i) along the riser tube, (ii) at the outlet pipe, (iii) top of the absorber plate, and (iv) bottom of the absorber plate at 11:00 h for mass flow rate of 0.025 kg s^{-1} are presented in Fig. 8(a)–(d), respectively.

The variation of water temperature along the riser pipe length at 11:00 h, shown in Fig. 8(a), indicates higher outlet water temperature at the upper portion of the collector compared to the lower portion. This is expected since the inlet water absorbs heat as it moves upward through the riser tube. Fig. 8(b) shows the variation of temperature across the outlet tube diameter at 11:00 h. The temperature at the tube surface is 13 K higher than at the center. Since one side of the tube is brazed with the hot absorber plate, the

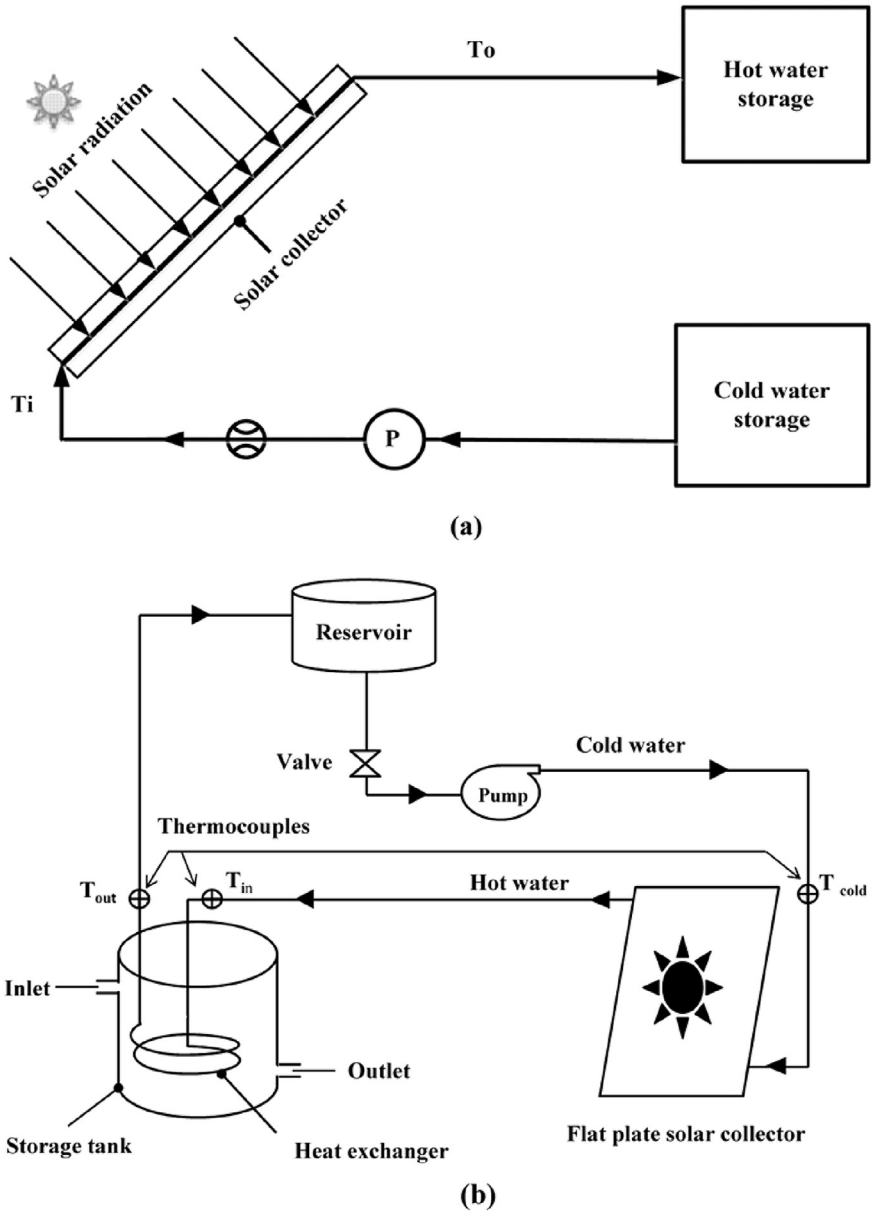

Fig. 2. Schematic diagrams of the experimental setup for water heating collector (a) open loop and (b) closed loop.

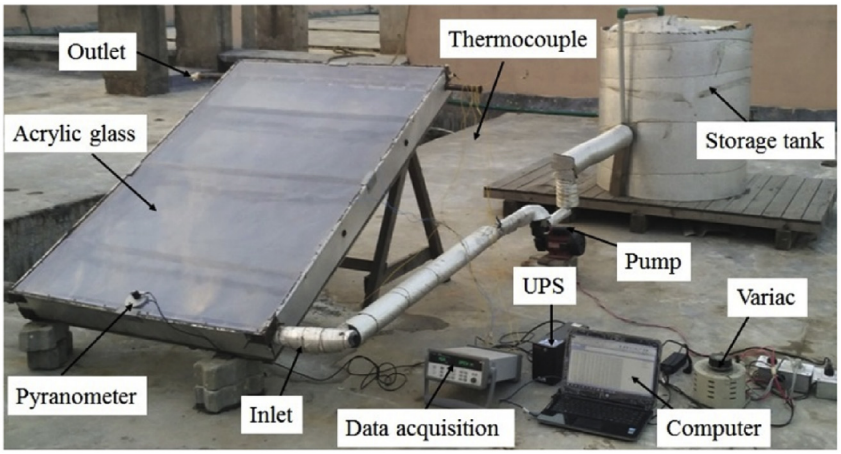

Fig. 3. Photograph of the open loop solar heating system.

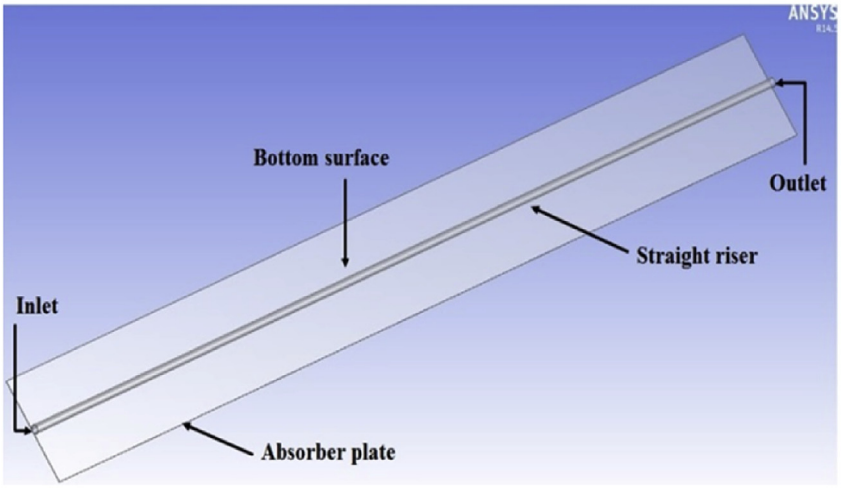

Fig. 4. Model geometry of the computational domain.

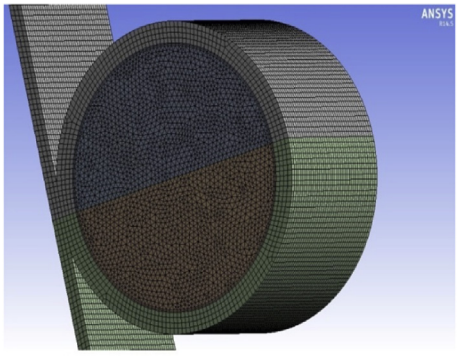

Fig. 5. Magnified meshed part of the computational domain.

temperature distribution at one side of the tube is higher compared to the other side. The heat transfer taking place is by a sequence of radiation, conduction through the tube thickness followed by convection inside the tube. Since it takes more time for the heat flow to reach the center of the tube by convection, the water temperature at the center of the tube is lower than at the surface. Fig. 8(c) and (d) show the variation of temperature at the top and bottom surface of the absorber plate. The temperature variation across the absorber plate length indicates a difference of 25 K between the inlet side and outlet side of the plate. Since heat is absorbed by the cold fluid flowing through the riser tube which is in contact with the absorber plate at the mid width section there is a variation of around 5 K across the plate width.

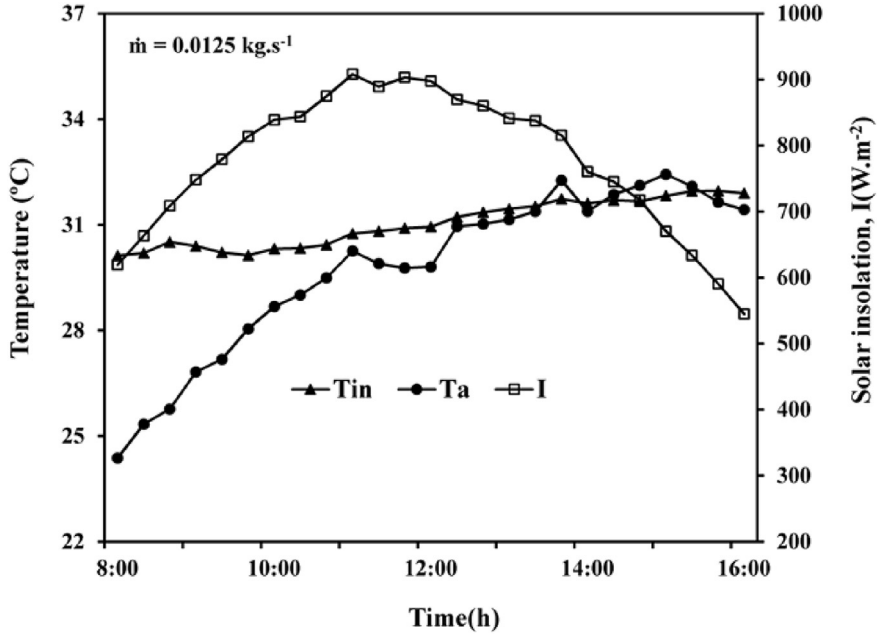

Fig. 6. Variation of inlet water temperature, ambient temperature and solar insolation vs time for $\dot{m} = 0.0125$ kg s^{-1}.

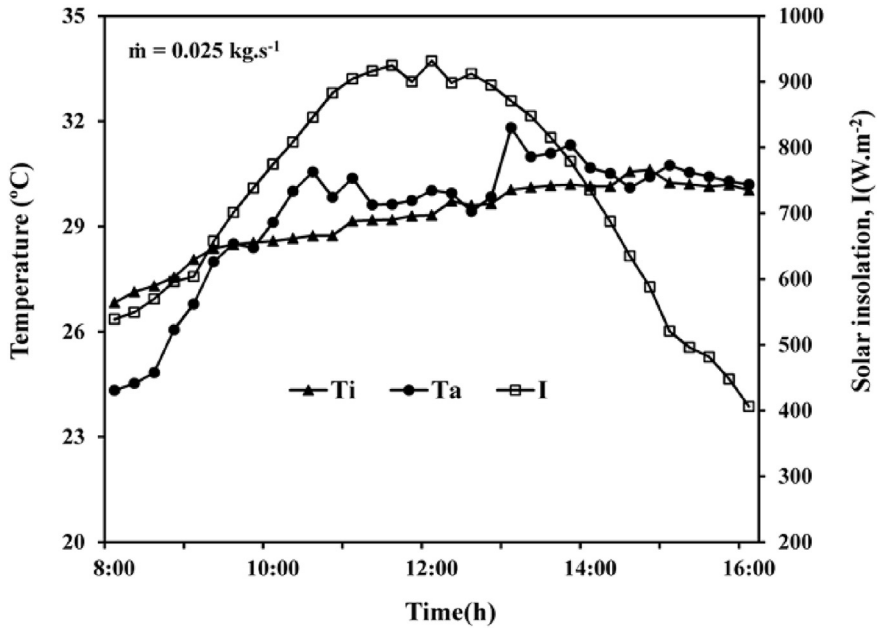

Fig. 7. Variation of inlet water temperature, ambient temperature and solar insolation vs time for $\dot{m} = 0.025$ kg s^{-1}.

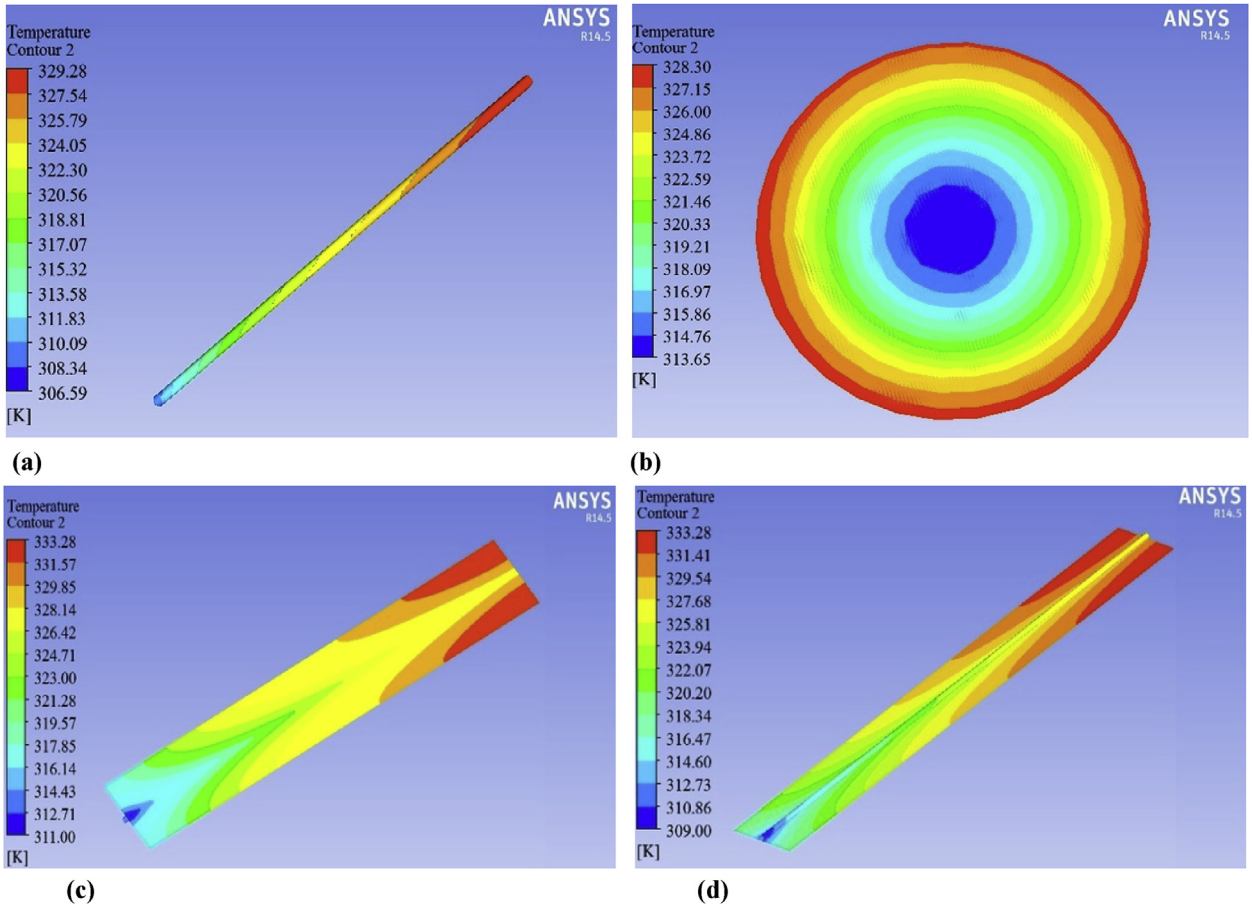

Fig. 8. (**a**). Variation of water temperature along the riser pipe at 11:00 h. (**b**). Simulated water temperature at the outlet pipe at 11:00 h. (**c**). Simulated absorber plate at the top surface at 11:00 h. (**d**). Simulated absorber plate at the bottom surface at 11:00 h.

2.2. Comparison of CFD predicted outlet water temperature, and absorber plate temperature with experimental data

Plots of experimental and simulation results of outlet water temperatures for mass flow rates of 0.0125 kg s^{-1} and 0.025 kg s^{-1} respectively, are shown in Fig. 9(a) and (b). The relative error between experimental results (X_{exp}) and simulation values (X_{sim}) is expressed by:

$$Error\ (\%) = \frac{|X_{sim.} - X_{exp.}|}{X_{sim.}} \times 100 \quad (6)$$

The maximum relative error of 5.2% and 4.4% for outlet water temperature obtained for mass flow rates of 0.0125 kg s^{-1} and 0.025 kg s^{-1} respectively, indicates good agreement. The relative error obtained in the present study is lower as compared to the results of others [28,29].

Plots of experimental and simulation values of absorber plate temperatures vs time for the two water flow rates are shown in Fig. 10(a) and (b). The experimental values of plate temperature are higher than the simulation values for both flow rates. Since the simulation was based on the assumption of a perfect contact between the absorber plate and the tube, better heat transfer occurs between the plate and the tube compared to the actual case. Hence the simulated absorber plate temperature values are lower than that of the experimental values. The relative error obtained between experiments and simulation results on the surface of the absorber plate is less than 2%.

2.3. The measured results of closed loop solar heating system

The measured ambient temperature, inlet and outlet water temperatures, thermal efficiency and solar insolation of the closed loop solar water heating experimental test for mass flow rate of 0.0125 kg s^{-1} is depicted in Fig. 11.

The solar insolation received at the collector surface showed a parabolic path with peak value attaining during the mid-day and latter decreases as the time increases. The solar insolation increases

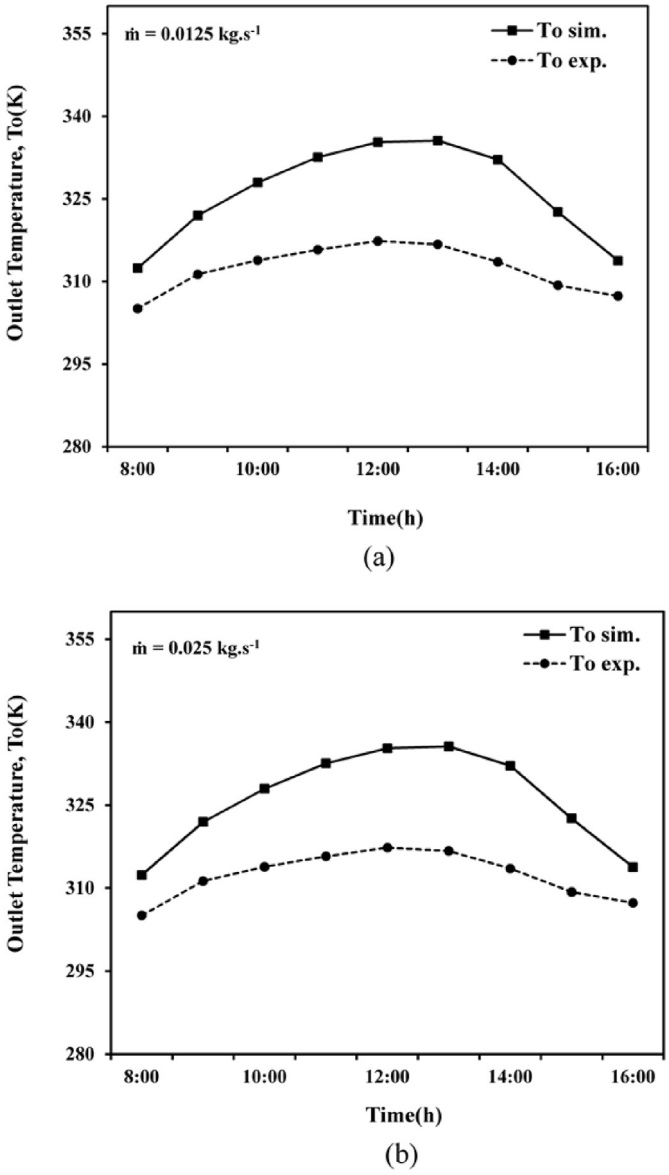

Fig. 9. Variation of predicted and experimental outlet water temperature vs time for (a) $\dot{m}$ = 0.0125 kg s^{-1}, and (b) $\dot{m}$ = 0.025 kg s^{-1}.

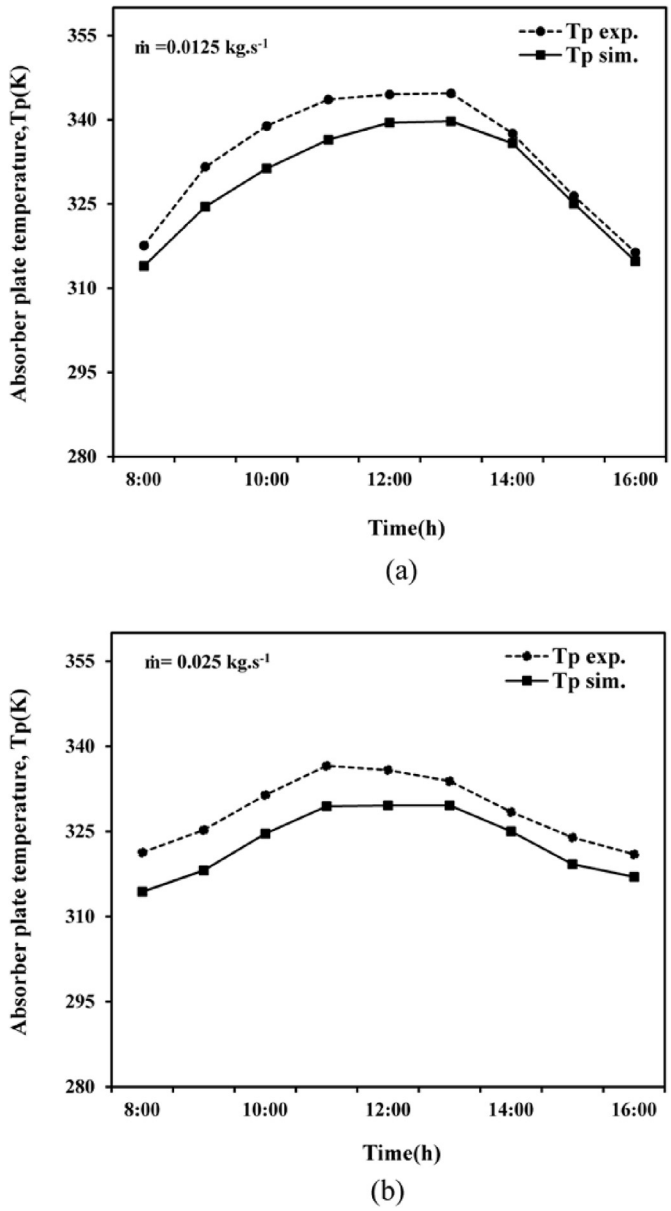

Fig. 10. Variation of predicted and experimental plate temperature vs time at (a) $\dot{m}$ = 0.0125 kg s^{-1}, and (b) $\dot{m}$ = 0.025 kg s^{-1}.

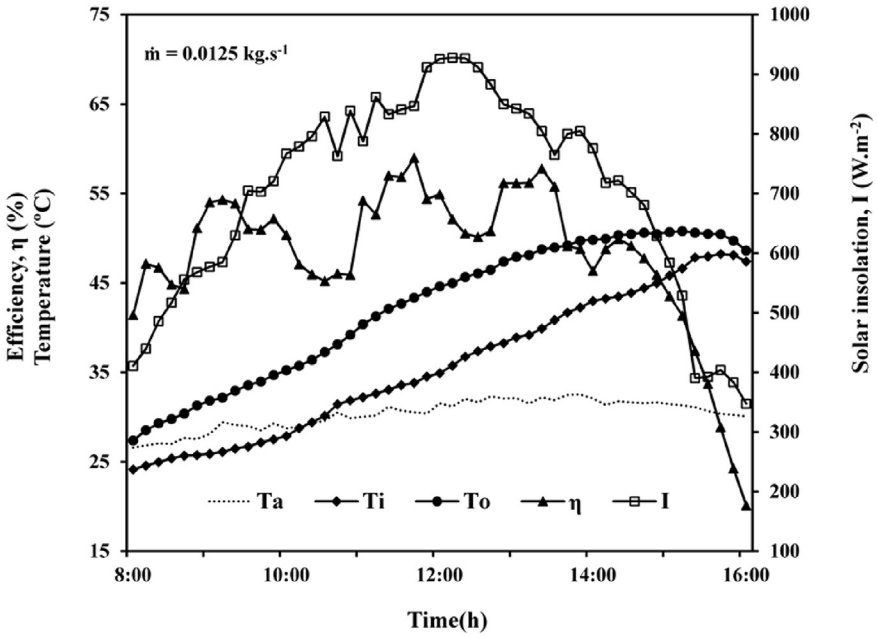

Fig. 11. The measured results of closed loop solar heating collector vs time.

from the morning, reaches its maximum value of 928 W m^{-2} at 12:30 h. The ambient temperature increases from 8:00 h and reaches the maximum value at 14:00 h. Similarly, the inlet water temperature increases from 24 °C at the morning and reaches peak value of 47.8 °C at 16:00 h. The outlet water temperature increased slowly from 8:00 h to 10:00 h due to the increase in solar irradiance and ambient temperature. Subsequently, both the inlet and outlet water temperature increased almost linearly from 10:00 h to 15:00 h and followed the same trend. Beyond 15:00 h, outlet water temperature reduced due to the decrease in solar irradiance, ambient temperature and increasing of inlet water temperature. This is mainly due to the higher energy loss from the solar heating system at higher inlet water temperature. The peak outlet water temperature of 50.8 °C is obtained for an inlet water temperature of 47.1 °C. The peak thermal efficiency of 59% is attained at 11:40 h. The thermal efficiency decreases continuously beyond 14:00 h. This was expected since the water temperature decrease due to the decrease in solar insolation for the same water flow rate and collector area. Beyond 16:00 h, the difference between the inlet and outlet water temperature is close to 0 K, due to lower solar insolation thereby reducing the thermal efficiency.

2.4. The measured results of open loop solar heating system

The thermal efficiency, inlet and outlet water temperatures, ambient temperature and solar insolation of the open loop solar

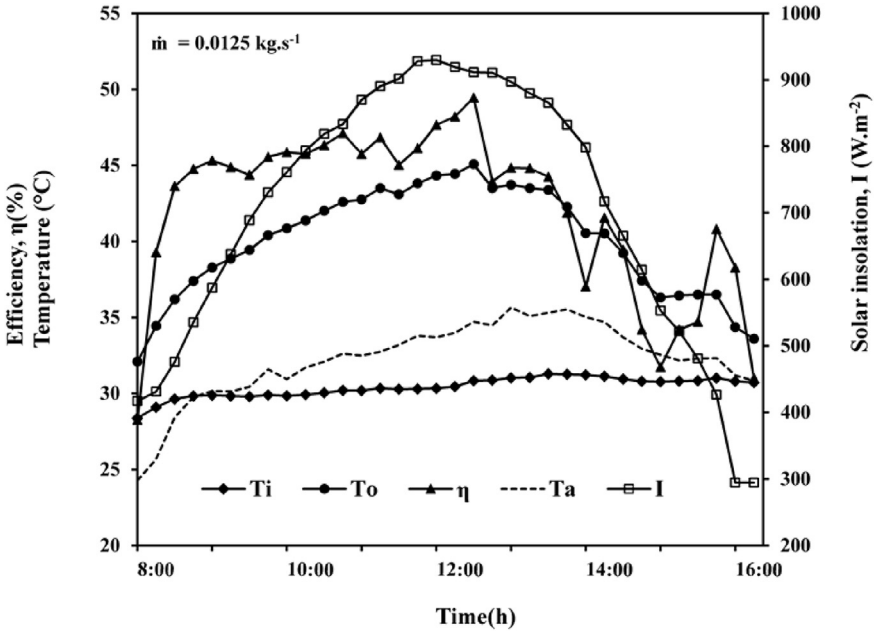

Fig. 12. The measured results of open loop solar heating collector vs time for $\dot{m} = 0.0125$ kg s^{-1}.

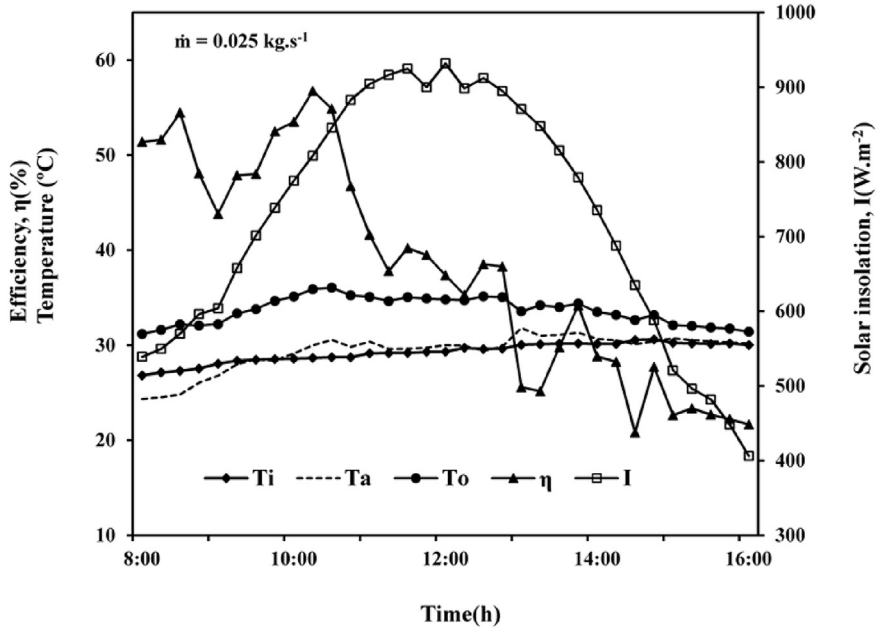

Fig. 13. The measured results of open loop solar heating collector vs time for $\dot{m} = 0.025$ kg s^{-1}.

collector for mass flow rate of 0.0125 kg s^{-1} and 0.025 kg s^{-1} are depicted in Figs. 12 and 13, respectively.

At flow rates of 0.0125 kg s^{-1} and 0.025 kg s^{-1}, the inlet water temperature increases by a maximum of 2 °C and 4 °C due to the increment of solar insolation and ambient temperature. As result of this, the thermal efficiency increases. This is due to the insulation provided to the cold water storage tank in order to increase the heat removal rate thereby reducing the energy loss from the solar collector.

Literature regarding closed loop solar water heating systems indicates rapid decrement in thermal efficiency for the flat plate collector at conditions of peak solar radiation due to higher energy loss. This can be attributed to the rise in inlet water temperature due to high solar insolation and ambient temperature during the peak conditions. In the present investigation, peak collector efficiencies of 49.7% and 56% are obtained for water flow rates of 0.0125 kg s^{-1} and 0.025 kg s^{-1}, respectively.

The variation of the outlet water temperature with time follows almost the same trend as the collector efficiency. The higher efficiency is obtained for higher mass flow rate whereas higher outlet temperature is obtained for lower flow rate, since the fluid is retained in the riser tubes for longer period. The outlet water temperature increased slowly from 8:00 h to 10:00 h due to the lower solar irradiance and ambient temperature. The maximum outlet water temperature of 45.1 °C and 36 °C and inlet water temperatures of 30.8 °C and 28.7 °C are obtained for flow rates of 0.0125 kg s^{-1} and 0.025 kg s^{-1}, respectively.

2.5. Temperature difference between outlet and inlet water for open loop solar heating system

The variation of difference in hot water and cold water temperature (ΔT) with time for open loop heating system for mass flow rates of 0.0125 kg s^{-1} and 0.025 kg s^{-1} is illustrated in Fig. 14.

The temperature difference is higher for lower mass flow rates. With higher water flow rate through the collector, the heat transferred per unit volume of water is lower and hence temperature difference between the inlet and outlet water decreases. At water flow rates of 0.0125 kg s^{-1} and 0.025 kg s^{-1}, the respective maximum change in water temperature (ΔT) are 14.5 K and 7.3 K. However, in closed loop solar heating system, the inlet water temperature and outlet water temperature increases continuously due to the increase in solar radiation and ambient temperature thereby reduces the change in water temperature.

2.6. Parametric study

Based on the simulation, parametric studies on the performance of the solar collector for various input conditions, *viz*., inlet water temperature, ambient temperature, water flow rate and solar insolation were carried out.

Fig. 15 shows the variation of collector efficiency and outlet water temperature vs inlet water velocity for 30 °C inlet water

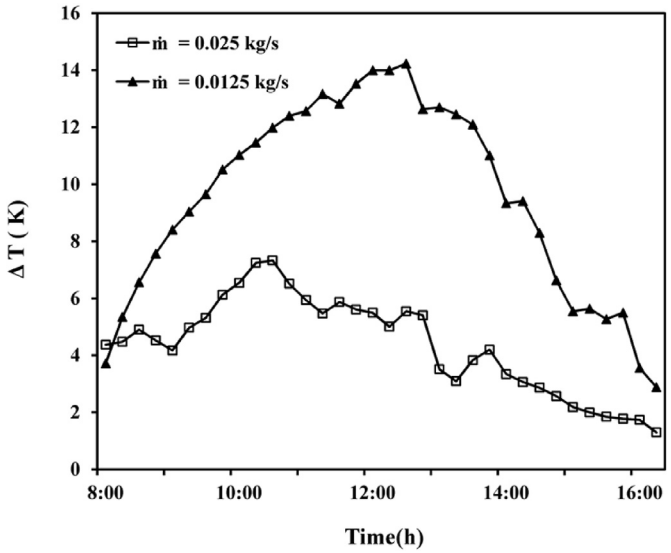

Fig. 14. Plot of temperature difference vs time for open loop collector.

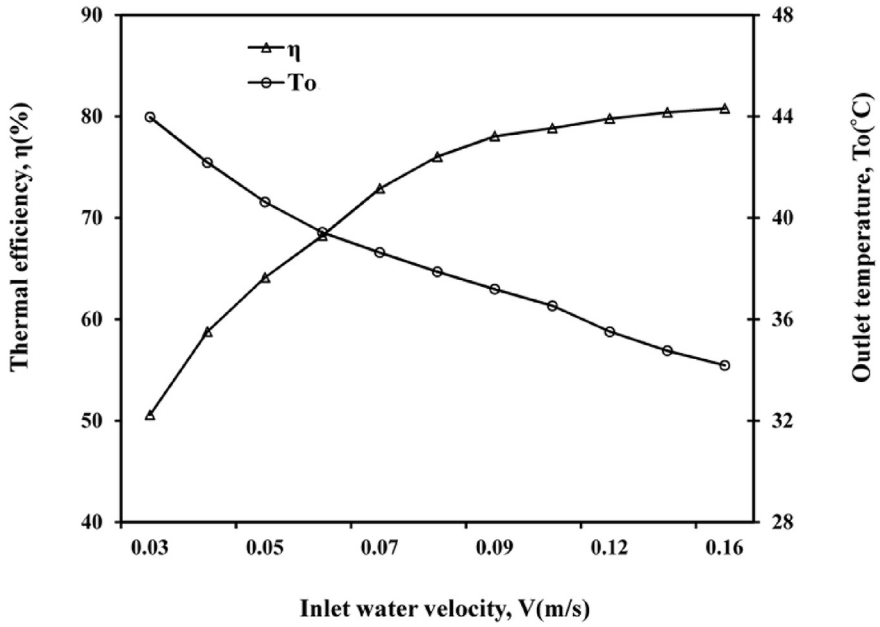

Fig. 15. Plot of thermal efficiency and outlet water temperature vs inlet water velocity.

temperature, 25 °C ambient temperature, and solar insolation of 700 W m^{-2}. The outlet water temperature decreases from 46 °C to 31 °C and collector thermal efficiency increases from 50.7% to 79.0% as the water velocity increases from 0.03 m s^{-1} to 0.16 m s^{-1}. With increase in water flow rate the heat transfer rate increases leading to decrease in the absorber plate temperature. This results in decrease in heat losses from the system with concomitant increase in thermal efficiency.

Plots of thermal efficiency and outlet water temperature vs solar insolation at water flow rate of 0.03 m s^{-1}, 25 °C ambient temperature and inlet water temperature of 30 °C is shown in Fig. 16.

Increasing the solar insolation from 150 W m^{-2} to 1050 W m^{-2} increases the thermal efficiency from 33% to 53% and outlet water temperature from 32 °C to 51.3 °C, respectively. The increase in solar insolation leads to increase in heat gain and collector heat transfer rate resulting in increase in the thermal efficiency and outlet water temperature.

Fig. 17 shows the plots of thermal efficiency and outlet water temperatures vs ambient temperature at inlet water temperature of 30 °C, inlet water velocity of 0.03 m s^{-1} and 700 W m^{-2} solar insolation. As the ambient temperature increases from 5 °C to 45 °C, the thermal efficiency and outlet water temperature increases from 32% to 66% and 38.7 °C–46.3 °C, respectively. It is evident from Eq. (7) that as the ambient temperature increases, the collector heat loss decreases thereby increases the thermal efficiency of the collector. In addition, with higher ambient temperature, the collector

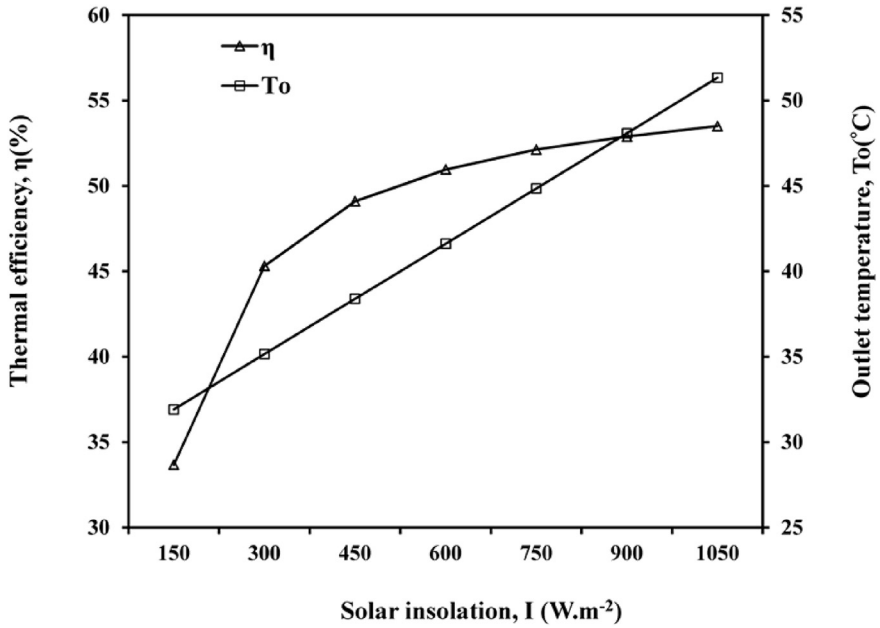

Fig. 16. Plot of thermal efficiency and outlet water temperature vs solar insolation.

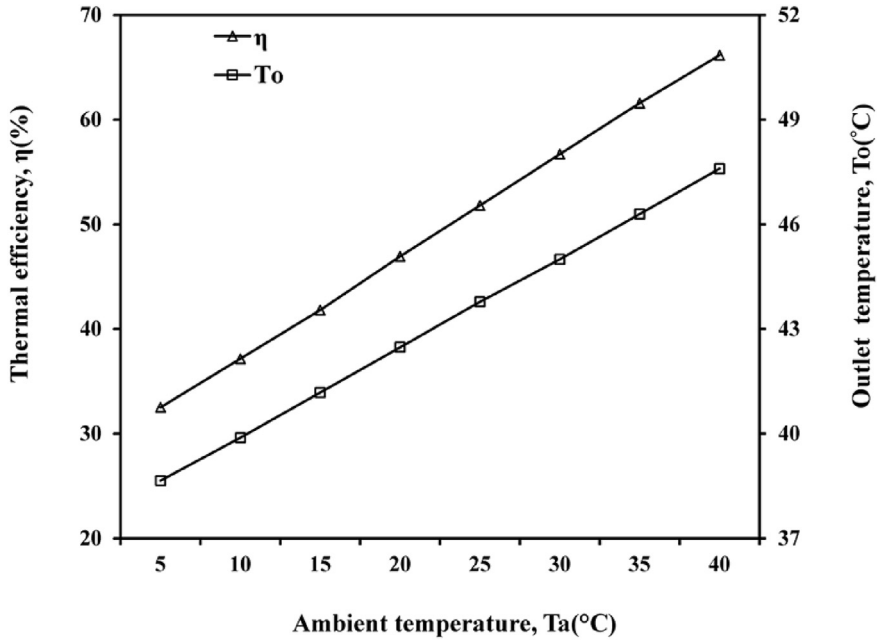

Fig. 17. Plot of thermal efficiency and outlet water temperature vs ambient temperature.

receives more heat from the solar radiation as well as from the surrounding atmosphere thus increases the outlet water temperature.

Variation of collector efficiency and outlet water temperature vs inlet water temperature at an inlet water velocity of 0.03 m s^{-1}, ambient temperature of 25 °C and solar insolation of 700 W m^{-2} are shown in Fig. 18.

As the inlet water temperature increases from 15 °C to 45 °C, the thermal efficiency of the collector decreases from 61.5% to 37.3% whereas the outlet water temperature increases from 36.3 °C to 54.9 °C. At higher inlet water temperature, the ΔT decreases, and hence decreases the thermal efficiency.

The most important component in solar flat plate collectors is the absorber plate, where the solar energy is absorbed and transferred to the fluid medium. The material properties of absorber plate and riser tubes play an important role in heat transfer characteristics of the solar collector.

The effect of energy loss parameter $((Ti-Ta)/I)$ on the thermal efficiency of the collector was investigated by varying the inlet water temperature from 15 °C to 45 °C, using copper, aluminum and steel as an absorber plate materials. Fig. 19 shows the results obtained for an inlet water velocity of 0.03 m s^{-1}, ambient temperature 25 °C and solar insolation 700 W m^{-2}.

The figure indicates that the thermal efficiency of the collector

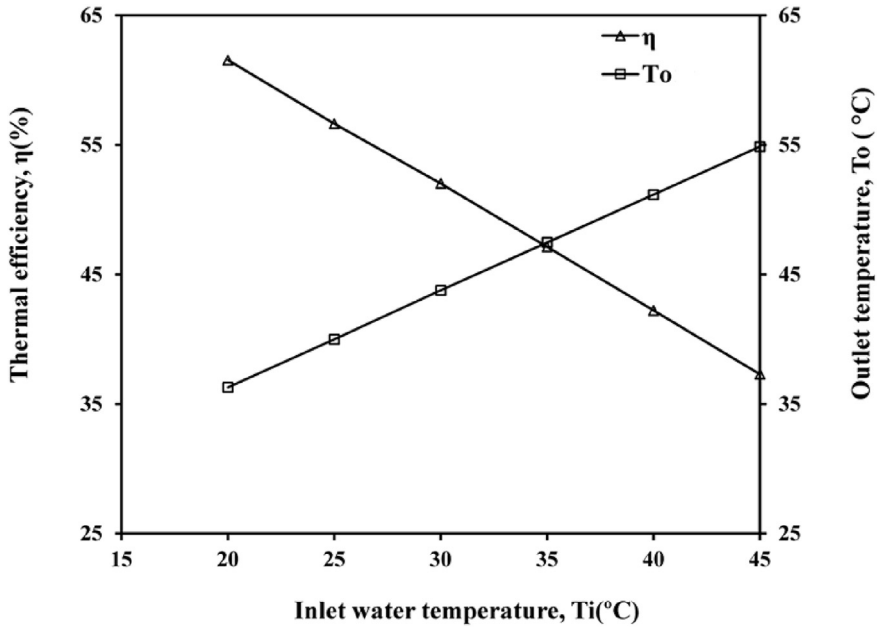

Fig. 18. Plot of thermal efficiency and outlet water temperature vs inlet water temperature.

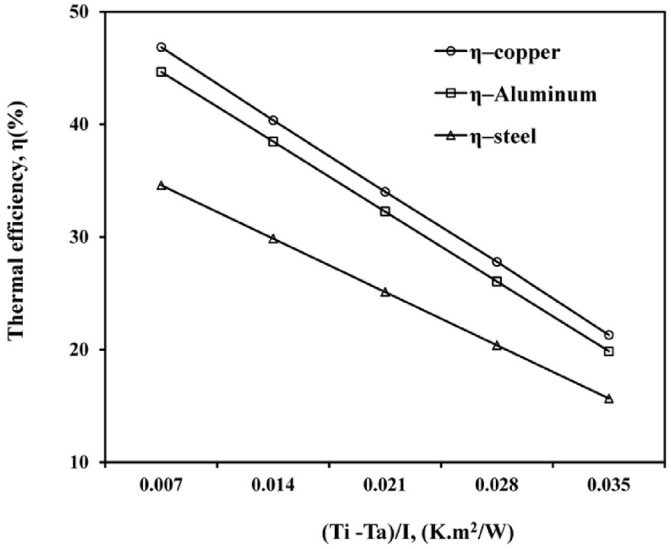

Fig. 19. Plot of thermal efficiency vs absorber plate material.

decreases with increase in heat loss parameter for all the materials. Higher thermal efficiency is obtained when copper is used as the plate material whereas the least efficiency is obtained with steel as the plate material. This is due to the higher thermal conductivity of copper compared to aluminum and steel. The thermal efficiency of the collector is only 2% less with aluminum as the plate material compared to copper. Use of aluminum as the plate material may be a better option compared to copper in terms of weight and cost of the collector.

2.7. Instantaneous efficiency of the closed loop solar heating collector

The efficiency of the solar collector is affected by the input conditions, *viz*., ambient temperature (*Ta*), solar insolation (*I*) and the mean temperature (*Tm*) of water across the collector. The main parameter used to evaluate the performance of the solar heating system is collector energy loss factor ((*Tm*−*Ta*)/*I*) expressed by Ref. [30]:

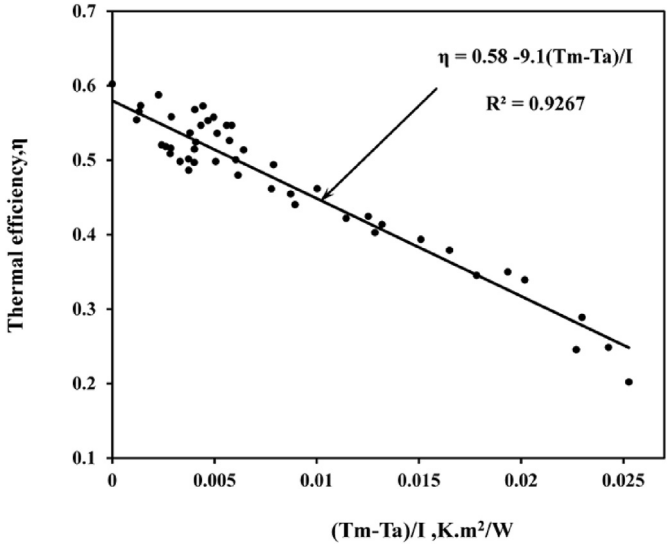

Fig. 20. η vs (Tm−Ta)/I relation for the closed loop solar heating collector.

$$\eta = \eta_0 - \alpha_0 \frac{(Tm - Ta)}{I} \tag{7}$$

The intercept η_0 represents the thermal efficiency of the collector at zero reduced temperature and slope α_0 represents the energy loss coefficient of the solar collector. Fig. 20 shows the plots of η vs $(Tm-Ta)/I$ for the closed loop solar heating collector. The data points fitted with a straight line relationship is expressed by Eq. (8) with a regression coefficient (R^2) of 0.927.

$$\eta = 0.58 - 9.1 \frac{(Tm - Ti)}{I} \tag{8}$$

3. Conclusions

Experimental investigation on the performance of a flat plate solar collector was carried out in this study. A CFD model of a flat plate solar collector with single riser tube and absorber plate is developed at steady state condition. The flow rate taken in each riser tube was 1/10th of the total flow rate in the header. Comparison of the simulation results with the experimental data reveals that the model could predict the outlet water and absorber plate temperatures within a maximum relative error of 5.4% and 2%, respectively. Parametric study using the CFD model reveals the following:

a. The thermal efficiency of the collector increases with increase in water flow rate, solar insolation, ambient temperature, conductivity of the absorber plate material and decrease in inlet water temperature.
b. Since the performance is reduced only marginally, aluminum would be a better option as an absorber plate material in terms of light weight and cost compared to copper.
c. The change in water temperature was higher for the open loop heating system compared to closed loop heating system.

Nomenclatures

h_b	Convective heat transfer coefficient of the bottom surface, $W.m^{-2}.K^{-1}$
V_w	Wind speed, $m.s^{-1}$
V	Inlet water velocity, $m.s^{-1}$
I	Solar insolation, $W.m^{-2}$
Q_i	Heat energy absorbed by the solar collector, W
A_c	Effective collector area, m^2
η	Thermal efficiency
η_0	Thermal efficiency of collector at zero reduced temperature
α_0	Energy loss coefficient
Q	Heat absorbed by the water, kJ
$\dot{m}$	Mass flow rate, kg/s
c_p	Specific heat of water, kJ/kg. K
Ti	Inlet water temperature, K
To	Outlet water temperature, K
Ta	Ambient temperature, K
Tm	Mean temperature, K
Tp	Absorber plate temperature, K
ΔT	Change in water temperature, K
X_{exp}	Experimental value
X_{sim}	Simulated value

Greek symbols

α	absorptivity

τ transmissivity

Subscripts

b bottom

w wind

References

[1] M. Keyanpour-Rad, et al., Feasibility study of the application of solar heating systems in Iran, Renew. energy 20.3 (2000) 333–345.

[2] R. Banos, F. Manzano-Agugliaro, F.G. Montoya, C. Gil, A. Alcayde, J. Gómez, Optimization methods applied to renewable and sustainable energy: a review, Renew. Sustain. Energy Rev. 15 (4) (2011 May 31) 1753–1766.

[3] E. Bilgen, B.J.D. Bakeka, Solar collector systems to provide hot air in rural applications, Renew. Energy 33 (2008) 1461–1468.

[4] H. Dagdougui, A. Ouammi, M. Robba, R. Sacile, Thermal analysis and performance optimization of a solar water heater flat plate collector: application to Tétouan (Morocco), Renew. Sustain. Energy Rev. 15 (1) (2011 Jan 31) 630–638.

[5] S. Janjai, A. Esper, W. Mühlbauer, Modelling the performance of a large area plastic solar collector, Renew. energy 21 (3) (2000 Nov 1) 363–376.

[6] Soteris Kalogirou, Thermal performance, economic and environmental life cycle analysis of thermosiphon solar water heaters, Sol. energy 83.1 (2009) 39–48.

[7] Soteris A. Kalogirou, Flat-plate collector construction and system configuration to optimize the thermosiphonic effect, Renew. Energy 67 (2014) 202–206.

[8] M. Madhusudan, G.N. Tiwari, D.S. Hrishikeshan, H.K. Sehgal, Optimization of heat losses in normal and reverse flat-plate collector configurations: analysis and performance, Energy Convers. Manag. 21 (3) (1981 Dec 31) 191–198.

[9] D. Njomo, M. Daguenet, Sensitivity analysis of thermal performances of flat plate solar air heaters, Heat mass Transf. 42 (12) (2006 Oct 1) 1065–1081.

[10] N. Madhukeshwara, E.S. Prakash, An investigation on the performance characteristics of solar flat plate collector with different selective surface coatings, Int. J. Energy & Environ. 3 (1) (2012 Jan 1).

[11] B. Prakash, B. Jaya, Vishnuprasad, V. Venkata Ramana, Performance study on effect of nano coatings on liquid flat plate collector: an experimental approach, Int. J. Mech. Eng. Rob. Res. 2 (4) (2013) 379–384.

[12] E. Zambolin, D. Del Col, Experimental analysis of thermal performance of flat plate and evacuated tube solar collectors in stationary standard and daily conditions, Sol. Energy 84.8 (2010) 1382–1396.

[13] Hoyt Hottel, B. Woertz, Performance of flat-plate solar-heat collectors, Trans. ASME Am. Soc. Mech. Eng. United States 64 (1942).

[14] J.A. Duffie, W.A. Beckman, Solar Engineering of Thermal Processes, Wiley third ed., New York etc., 2006.

[15] R.S. Gorla, Finite element analysis of a flat plate solar collector, Finite Elem. Anal. Des. 24 (4) (1997 Feb 20) 283–290.

[16] N. Akhtar, S.C. Mullick, Effect of absorption of solar radiation in glass-cover (s) on heat transfer coefficients in upward heat flow in single and double glazed flat-plate collectors, Int. J. Heat Mass Transf. 55 (1) (2012 Jan 15) 125–132.

[17] S. Lecoeuche, S. Lalot, Prediction of the daily performance of solar collectors, Int. Commun. heat mass Transf. 32 (5) (2005 Apr 30) 603–611.

[18] E.H. Amer, J.K. Nayak, G.K. Sharma, Transient method for testing flat plate solar collectors, Energy Convers. Manag. 39 (7) (1998), 549 e 558.

[19] Adnan Shariah, Bassam Shalabi, Optimal design for a thermosyphon solar water heater, Renew. energy 11.3 (1997) 351–361.

[20] T. Sultana, G.L. Morrison, G. Rosengarten, Thermal performance of a novel rooftop solar micro-concentrating collector, Sol. Energy 86 (7) (2012 Jul 31) 1992–2000.

[21] M. Selmi, M.J. Al-Khawaja, A. Marafia, Validation of CFD simulation for flat plate solar energy collector, Renew. Energy 33 (3) (2008 Mar 31) 383–387.

[22] K.P. Gertzos, S.E. Pnevmatikakis, Y.G. Caouris, Experimental and numerical study of heat transfer phenomena, inside a flat-plate integrated collector storage solar water heater (ICSSWH), with indirect heat withdrawal, Energy Convers. Manage 49 (11) (2008) 3104–3115.

[23] M.B. Gadi, Design and simulation of a new energy-conscious system (CFD and solar simulation), Appl. Energy 65 (1–4) (2000) 251–256.

[24] G. Martinopoulos, D. Missirlis, G. Tsilingiridis, K. Yakinthos, N. Kyriakis, CFD modeling of a polymer solar collector, Renew. Energy 35 (7) (2010 Jul 31) 1499–1508.

[25] H. Al-Ansary, O. Zeitoun, Numerical study of conduction and convection heat losses from a half-insulated air-filled annulus of the receiver of a parabolic trough collector, Sol. Energy 85 (11) (2011 Nov 30) 3036–3045.

[26] Jorge Facão, Optimization of flow distribution in flat plate solar thermal collectors with riser and header arrangements, Sol. Energy 120 (2015) 104–112.

[27] William H. MacAdams, William H. McAdams, Heat Transmission, McGraw-Hill, New York, 1954.

[28] I. Attar, A. Farhat, Efficiency evaluation of a solar water heating system applied to the greenhouse climate, Sol. Energy 119 (2015) 212–224.

[29] H. Taherian, et al., Experimental validation of dynamic simulation of the flat plate collector in a closed thermosyphon solar water heater, Energy Convers. Manag. 52.1 (2011) 301–307.

[30] X.D. Zhao, Z.Y. Wang, Q. Tang, Theoretical investigation of the performance of a novel loop heat pipe solar water heating system for use in Beijing, China, Appl. Therm. Eng. 30 (2010) 2526–2536.